Effects of Microcrystallinity and Morphology on Physical Aging of Poly(ethylene terephthalate)

Hongxia Zhou,[1*] Elizabeth A. Lofgren,[1] Saleh A. Jabarin[1,2]

[1]*Polymer Institute, The University of Toledo, Toledo, Ohio 43606-3390*
[2]*Department of Chemical and Environmental Engineering, College of Engineering, The University of Toledo, Toledo, Ohio 43606-3390*

Received 5 March 2007; accepted 27 April 2007
DOI 10.1002/app.26779
Published online 22 August 2007 in Wiley InterScience (www.interscience.wiley.com).

ABSTRACT: Physical aging characteristics of poly(ethylene terephthalate) have been evaluated in relationship to volume fraction levels of crystallinity up to 25%. Changes in the enthalpies of relaxation, monitored at aging temperatures from 55 to 65°C, are found to give good fits with the Cowie-Ferguson model. Overall equilibrium enthalpy of relaxation values decrease linearly with increased crystallinity. They increase with decreased aging temperature, providing extrapolated lower temperature results that are validated in terms of specific heat relationships. Activation energies for enthalpic relaxations are found to increase from 337 to 361 kJ/mole as crystallinity increases up to 25%. Overall relaxation endotherms are further resolved into contributions from interspherulitic and intraspherulitic amorphous regions. Interspherulitic, equilibrium enthalpies of relaxation decrease with increased levels of crystallinity, while intraspherulic values show corresponding increases. Characteristic relaxation times of the intraspherulic regions increase greatly, as levels of crystallinity increase; however, interspherulitic relaxation times decrease very slightly. Dynamic differential scanning calorimetry results show two glass transitions in the case of a 25% crystalline sample and a single transition for noncrystallized material. © 2007 Wiley Periodicals, Inc. J Appl Polym Sci 106: 3435–3443, 2007

Key words: poly(ethylene terephthalate); physical aging; crystallinity; enthalpy of relaxation; relaxation time

INTRODUCTION

The phenomena of physical aging have been studied extensively in amorphous poly(ethylene terephthalate) (PET) and results are well documented.[1–14] Additional studies have been reported describing the behavior of semicrystalline PET.[15–24] The effects of physical aging on mechanical properties and environmental stress crack resistance have also been investigated by others[1,2,11] as well as in our laboratories.[10,12,25–32] Previous systematic polyester studies at the Polymer Institute have included aging effects on physical properties and environmental stress cracking behaviors of amorphous homopolymers,[10,12] copolymers,[12,25,26] blends[12,27] and oriented PET.[12,28–31] The objectives of the current investigations are to evaluate aging effects on physical properties and environmental stress cracking behaviors of semicrystalline PET, with emphasis on low levels of crystallinity (within the range up to 25%). In this article, we present results of the physical aging characterization of the semicrystalline PET. An additional paper is in progress, describing the relationships among physical aging, mechanical properties, and the environmental stress crack resistance of the semicrystalline PET.

While previous studies have correlated the overall effects of crystallinity with the enthalpies of relaxation and relaxation times, the current study seeks to further evaluate the specific effects of different levels of crystallinity on the amorphous phases inside and outside the spherulites. For this purpose, our study utilized samples quiescently crystallized at 115°C, to attain levels of crystallinity up to 25%. Samples crystallized for different times at a given temperature, exhibit similar modes of crystallization and growth. With increasing exposure times, their spherulites increase in size and number. For this reason, samples can be prepared with various distributions of amorphous materials, both outside (interspherulitic) and within (intraspherulitic or inter-lamellar) the spherulites. Such a series of samples permits evaluations of materials with substantially amorphous characteristics, through a range in which spherulites have formed at increasing levels of crystallinity in a continuous amorphous phase. As sample crystallinity increases, the spherulites begin to impinge and their growth reduces the interspherulitic amorphous phase,

Correspondence to: S. A. Jabarin (saleh.jabarin@utoledo.edu).
**Present address:* Tulane University, New Orleans, Louisiana.

Contract grant sponsor: PET Industrial Research Consortium.

© 2007 Wiley Periodicals, Inc.
WILEY InterScience® DISCOVER SOMETHING GREAT

while correspondingly larger amorphous regions reside within the spherulites. At levels of crystallinity exceeding 25%, spherulitic impingement is present and some secondary crystallization may also occur. The purpose of the current work has been to investigate changes in aging behavior of PET within a range of crystallinity that has commercial significance. Nonoriented PET materials frequently achieve low levels of thermally induced crystallinity during production and subsequently experience aging related problems in terms of impact failures and/or environmental stress cracking.

Samples prepared in the range from 0 to 25% crystallinity were held at aging temperatures from 55 to 65°C and periodically evaluated in terms of changes in enthalpy of relaxation or free volume recovery, recorded during differential scanning calorimetry. This aging temperature range was chosen to be well below the glass transition and crystallization temperatures of PET, but to be high enough to attain equilibrium conditions during physical aging. Initial evaluations characterized changes in terms of overall relaxation behavior in relationship to levels of crystallinity and exposure temperatures. Physical aging results were then further resolved to describe relative influences of the interspherulitic as well as intraspherulitic amorphous components on their corresponding enthalpies of relaxation, equilibrium relaxation values, and characteristic relaxation times.

EXPERIMENTAL

Evaluated materials were commercially extruded sheet with thickness values from 0.25 to 0.38 mm. The sheet was prepared from Eastman 9921 PET copolymer with an intrinsic viscosity of 0.8 dL/g, corresponding to a number average molecular weight (M_n) of 26,000 and containing 3.5 mol % cyclohexane dimethanol (CHDM). All samples were exposed to 85°C for 15 min to remove residual stress and previous aging history, before further treatment or evaluation. Various levels of crystallinity were achieved as a result of controlled exposure times in a 115°C circulating air oven.

Sample densities were determined at 25°C according to ASTM procedure D-1505. The density gradient column was prepared from aqueous calcium nitrate solutions and calibrated with glass beads of known densities. Accuracy was within ± 0.0003 g/cm^3. Volume fraction crystallinity (X_c) was calculated from sample density (ρ) values according to:

$$X_c = (\rho - \rho_a)/(\rho_c - \rho_a) \quad (1)$$

The amorphous density (ρ_a) of this copolymer was taken as 1.323 g/cm^3 (Ref. 33) and that of the 100% crystalline material (ρ_c) as 1.455 g/cm^3 (Ref. 34).

Samples prepared at specified levels of crystallinity were exposed to aging temperatures of 55, 60, and 65°C in a circulating dry air oven. Portions of each material were removed periodically for evaluation, with a Perkin-Elmer (DSC-7) differential scanning calorimeter equipped with nitrogen purge. Standard DSC measurements were conducted at 10°C per min. Dynamic differential scanning calorimetry (DDSC) measurements utilized 35 repetitive heat cool cycles, with an underlying heating rate (B_0) of 1°C per minute, temperature amplitude (T_a) of 1.5°C, and a frequency (f_0) of 8.33 mHz. These parameters were calculated according to Refs. 12, 35, 36:

$$B_0 = \beta_1(T_3 - T_1)/2(T_2 - T_1) \quad (2)$$

$$T_a = 0.5[T_2 - (T_1 + T_3)/2] \quad (3)$$

$$f_0 = \beta_1/2(T_2 - T_1) \quad (4)$$

where β_1 is the heating rate, T_1 is the initial temperature, T_2 is the temperature after heating, and T_3 is the temperature after cooling.

Small angle light scattering measurements were used to obtain values for the spherulitic radii of samples prepared with various levels of crystallinity. The apparatus consists of a Spectra Physics model 155 helium-neon gas laser ($\lambda_0 = 635.8$ nm), a rotatable polarizer, fixed analyzer, optical display panel, camera, and computer equipped with IMAQ.vi programs for LabVIEW 5.0. The four-leaf clover patterns were measured in the Hv scattering mode (with the polarizer and analyzer perpendicular to each other). Spherulitic radii were obtained according to Ref. 37:

$$4.1 = \frac{4\pi R}{\lambda} \sin \frac{\Theta \max}{2} \quad (5)$$

where λ is the wavelength of light in the scattering medium, R is the spherulite radius, and Θ max is the scattering angle where the intensity is maximum.

RESULTS AND DISCUSSION

Amorphous polymeric materials are known to exhibit decreased molecular mobility with decreased exposure temperature. When such a material is quickly cooled from the liquid, to a temperature (T_a) below its glass transition temperature (T_g), various kinetic constrains cause it to be in a nonequilibrium state, with excess enthalpy (H). As schematically illustrated in Figure 1,[12,38] at T_a the material has an initial enthalpy (H_a) shown as the thin solid line. If the material is held at T_a for a specific time, H_a will decrease to H_t, shown as the heavy solid line. If the material is cooled very slowly or held at T_a for an infinite time, H_a will further decrease to reach its equilibrium enthalpy

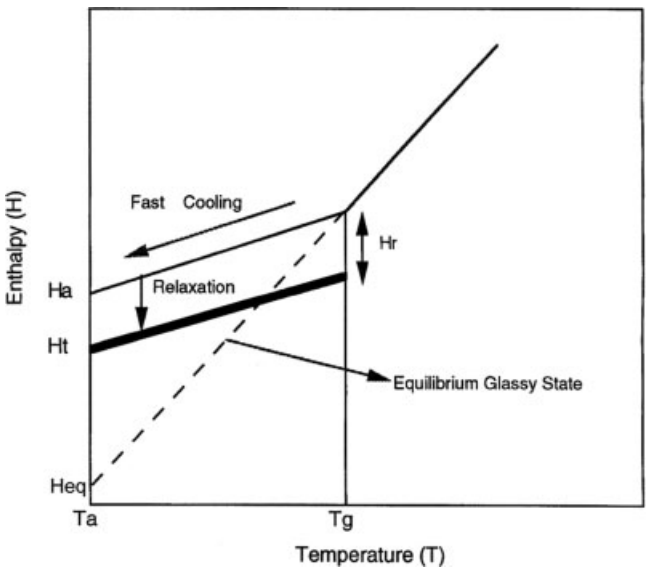

Figure 1 Schematic illustration, showing the relationship between PET aged in the glassy state and the relaxation endotherm, in terms of enthalpy versus temperature changes.

(H_{eq}), shown as the dashed line. As these changes occur, the molecular chains of the material relax toward a lower energy state, with decreased entropy or internal energy, releasing a small amount of heat. Materials that have been aged at T_a can be heated in a DSC to record the change in energy that has occurred during aging. The relaxation endotherm, which occurs near T_g, results from, and is proportional to recovery of the lost enthalpy or free volume. The size of the relaxation endotherm increases, with increased aging time. As aging temperatures approach T_g, these changes are more rapid; however, the equilibrium enthalpy values achieved at higher temperatures decrease as illustrated in Figure 1.

Samples prepared with volume fraction levels of crystallinity up to 25% were exposed to aging temperatures of 55, 60, and 65°C. They were then periodically monitored in terms of changes in their relaxation endotherm (ΔH) values. Figure 2 gives an example of the relationships observed at 65°C. Similar results were observed at 55 and 60°C. The overall enthalpies of relaxation are seen to increase with increasing aging times. Samples with higher crystalline fractions are found to exhibit smaller changes in their relaxation endotherm (ΔH) values, than those with larger amorphous contents. These differences are greater than can be accounted for by normalizing the data to 100% amorphous content. Even in the case of 25% crystalline samples, normalized values obtained after aging at 65°C would change only from 2.24 to 2.99 J/g. After 60°C aging, the increase would be from 3.09 to 4.12 J/g and after 55°C aging from 4.54 to 6.05 J/g. These normalized values are significantly lower than those obtained for equivalent noncrystallized materials. The observed differences result not only from reduction in overall amorphous component, but also from restrictions imparted by its location and distribution. All values are; therefore, reported as measured, in terms of the total sample mass, regardless of crystalline content.

To further describe the kinetics of physical aging, the Cowie-Ferguson model[12,39,40] was applied to the data as shown in Figure 2. This empirical equation has been used to describe enthalpic aging as a function of exposure time at a given temperature according to:

$$\Delta H(t_a, T_a) = \Delta H_{eq}(t_a)[1 - \phi(t_a)] \quad (6)$$

where:

$$\phi(t_a) = \exp[-(t_a/t_c)^{\beta}] \quad (7)$$

Values for ΔH (t_a, T_a) represent the enthalpy lost during sample aging for a given time (t_a) and temperature (T_a). The relaxation function term (ϕ (t_a)) describes the kinetics of the approach of the system to the equilibrium state. Nonlinear cure-fitting analysis can be used to determine values for the equilibrium enthalpy of relaxation [ΔH_{eq} (T_a)] at a given temperature, as well as the characteristic relaxation time (t_c), and the nonlinearity parameter (β).[12,39,40] Although the ΔH_{eq} values obtained with this model are somewhat limited by its dependence on the experimental time scale, the results give a good approximation of material characteristics.

Tables I–III give Cowie-Ferguson parameters obtained by modeling 55, 60, and 65°C relaxation data. In addition to the Cowie-Ferguson equilibrium relax-

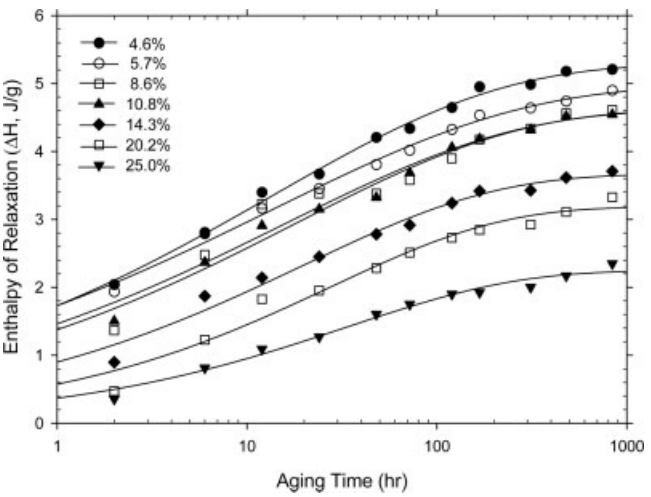

Figure 2 Changes in relaxation enthalpy, recorded for samples with levels of crystallinity up to 25%, are plotted as functions of aging times at 65°C.

TABLE I
Comparisons of Cowie-Ferguson Equilibrium Relaxation Endotherm (ΔH_{eq}) Parameters for Semicrystalline PET

Density (g/cm^3)	X_c (%)	ΔH_{eq} (J/g) 65°C	ΔH_{eq} (J/g) 60°C	ΔH_{eq} (J/g) 55°C	Extrapolated ΔH_{eq} (J/g) 50°C
1.3290	4.6	5.29	6.83	8.17	9.64
1.3305	5.7	4.97	6.23	7.81	9.18
1.3344	8.6	4.62	6.02	7.46	8.87
1.3372	10.8	4.63	5.78	7.12	8.33
1.3419	14.3	3.67	4.71	5.83	6.90
1.3496	20.2	3.18	4.19	5.34	6.40
1.3560	25.0	2.24	3.09	4.54	5.59

ation endotherm (ΔH_{eq}) values obtained at the evaluation temperatures, Table I also gives extrapolated values for 50°C exposures, since within a narrow temperature range the relationships between ΔH_{eq} values and aging temperatures are linear. This is consistent with behavior described in Figure 1. Figure 3 includes this 50°C data and illustrates the linear relationships between ΔH_{eq} values and volume fraction levels of crystallinity.

The validity of extrapolating equilibrium relaxation endotherm (ΔH_{eq}) values to lower temperatures was examined in terms of specific heat changes, recorded for noncrystallized (4.6%) and semi crystalline (20.2%) samples. As indicated in Figure 1, above T_g, enthalpy decreases linearly during cooling. In the glass transition region, there is a change in slope, because the polymer has excess enthalpy. At temperatures near and below T_g, physical aging and loss of enthalpy occur and values approach the extrapolated (dashed) line of Figure 1. The difference between the enthalpy of the glassy state and the equilibrium extrapolated line is ΔH_{eq}. If the calculated ΔH_{eq} values that were obtained either from the Cowie-Ferguson model or from lower temperature extrapolations are valid, the corresponding differences between H and ΔH_{eq} should fall on the extrapolated equilibrium line. At a given temperature (T), enthalpy (H) equals specific heat (C_p) times temperature or:

$$H = (C_p)(T) \tag{8}$$

Figure 4 gives an example of this behavior for material containing 20.2% crystallinity and with lower temperature values extended to 35°C. In this figure the filled points are obtained from eq. (8), while the unfilled points are calculated from eq. (8) minus ΔH_{eq}. It can be seen that the unfilled points fall on the extrapolated line, indicating the validity of the data.

The characteristic relaxation times (t_c) given on Table III have been plotted as functions of % crystallinity in Figure 5. As can be seen, t_c values increase with increased levels of sample crystallinity. Equivalent samples aged at lower temperatures, also exhibit higher t_c values. The slower aging behaviors, represented by larger t_c values, indicate that longer times are required for these samples to reach equilibrium conditions.

An Arrhenius type plot of ln t_c versus reciprocal aging temperature can be used to calculate the activation energy (E) required for enthalpic relaxation according to:

$$t_c = A \exp(E/RT)) \tag{9}$$

or

$$\ln t_c = \ln A + (E/R)(1/T) \tag{10}$$

where t_c is the characteristic relaxation time, T is the aging temperature (K), R is the gas constant (8.314 J/(deg mole) or 1.987 cal/(deg mole)), A is the frequency factor, and slope = E/R. A plot of this nature is shown in Figure 6 for uncrystallized sheet, aged at 55, 60, and 65°C. These data yield an activation energy of 337 kJ/mole. This figure also includes data taken from the literature[14,15] to illustrate the good correlation with results reported for other amorphous PET and obtained with modulated DSC measurements.

Aging data obtained for samples prepared at each level of crystallinity, were plotted in the manner described above to provide respective activation energy values given in Table III. As crystallinity increases from 4.6 to 25% activation energies increased from

TABLE II
Comparisons of Cowie-Ferguson Nonlinearity (β) Parameters for Semicrystalline PET

Density (g/cm^3)	X_c (%)	β 65°C	β 60°C	β 55°C
1.3290	4.6	0.36	0.37	0.30
1.3305	5.7	0.33	0.36	0.30
1.3344	8.6	0.35	0.36	0.32
1.3372	10.8	0.36	0.42	0.34
1.3419	14.3	0.43	0.40	0.32
1.3496	20.2	0.48	0.48	0.36
1.3560	25.0	0.49	0.44	0.39

TABLE III
Comparisons of Cowie-Ferguson Characteristic Relaxation Time (t_c) Parameters and Activation Energy Values for Semicrystalline PET

Density (g/cm^3)	X_c (%)	t_c (h)			Activation energy (kJ/mol)
		65°C	60°C	55°C	
1.3292	4.6	13.5	123	524	337
1.3305	5.7	13.6	141	571	344
1.3344	8.6	15.5	159	675	347
1.3372	10.8	17.7	186	789	350
1.3419	14.3	19.7	206	911	353
1.3496	20.2	27.9	298	1374	358
1.3560	25.0	33.9	366	1702	361

337 to 361 kJ/mole. This increased energy requirement can be explained by the more restrained chain mobility that results from increased levels of crystallinity.

Additional samples, crystallized to various levels, were monitored in terms of their spherulite radii using small angle light scattering. The relationship of average spherulitic radii to sample crystallinity is shown in Figure 7. It can be seen that changes in radii are greater as initial levels of crystallinity increase. At higher levels of crystallinity; however, change in the radii are much smaller. This takes place because at low levels of crystallinity, the spherulites are growing into amorphous regions of the polymer without any obstructions. As levels of crystallinity increase, the spherulites begin to impinge on one another, limiting radial increases. As this occurs, there is less interspherulitic amorphous material available for increased crystallization. After long exposure times at higher temperatures, amorphous material within spherulite can also be utilized for increased crystallinity. This changing distribution of amorphous polymer content is responsible for differences in aging behavior and for the two peaks recorded in the cases of some relaxation endotherms.

Previously described results have utilized the total relaxation endotherms, obtained while heating aged samples in a DSC. These results have been further resolved to describe aging behavior that occurs throughout the interspherulitic amorphous region (between the spherulites) as well as the intraspherulitic regions wihin them. Figure 8 gives an example of relaxation endotherms exhibited by samples that have undergone aging in both interspherulic and intraspherulitic amorphous regions. The size and distribution of these peaks changes with the crystalline content of the sample, as well as its aging history. The lower temperature peak (A_1) results from aging of the more mobile interspherulitic amorphous material and is most prevalent in samples with the lowest levels of crystallinity. Peak A_2 occurs at slightly higher temperatures and results from aging changes within the inter-lamellar amorphous regions of the spherulites. This peak, representing more restricted amorphous regions, is most prevalent among samples with higher levels of crystallinity.

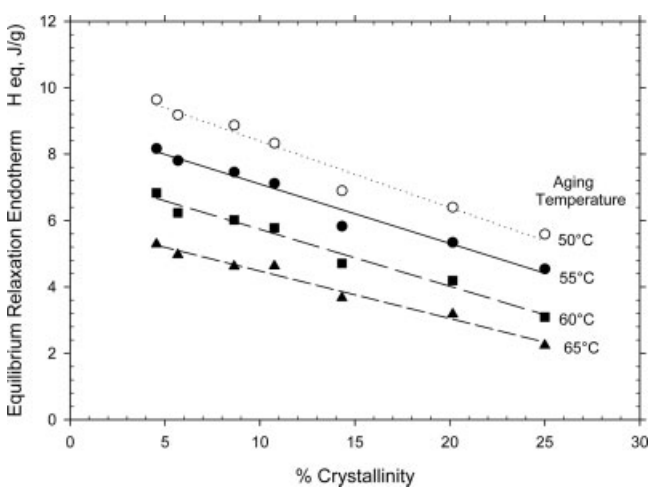

Figure 3 Equilibrium relaxation endotherm values are plotted as functions of % crystallinity for samples aged at 55–65°C. Extrapolated values for 50°C are included.

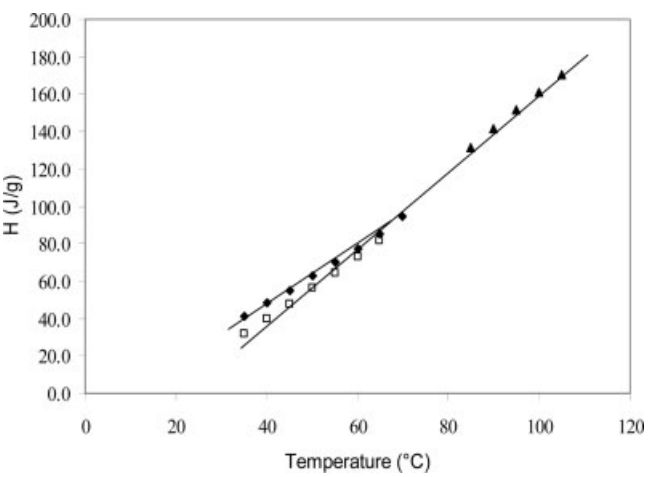

Figure 4 Measured (filled points) and calculated (open points) enthalpy values are plotted as functions of temperature for 20.2% crystalline material.

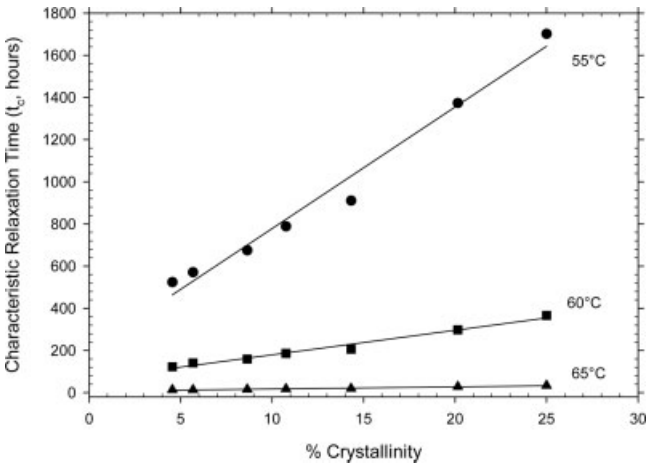

Figure 5 Characteristic relaxation time values, obtained with the Cowie-Ferguson model, are plotted as functions of % crystallinity for samples aged at 55–65°C.

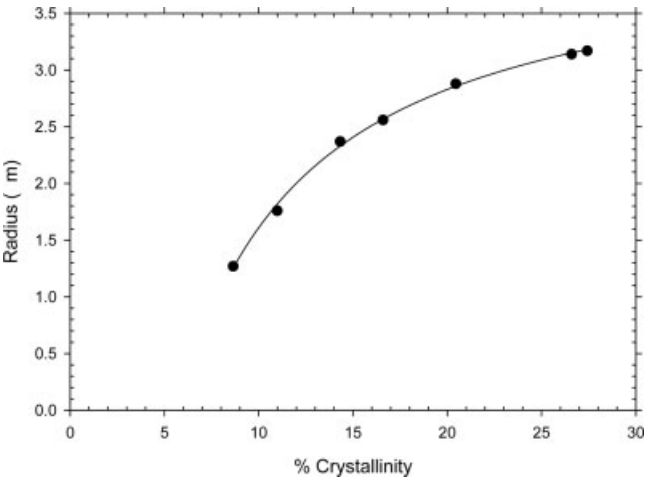

Figure 7 Average spherulite radii are plotted in relationship to overall levels of sample crystallinity.

The relative contributions to the relaxation process of the two amorphous regions have been evaluated in terms of areas enclosed by peaks A_1 and A_2. These calculations utilized the DSC partial area program supplied by Perkin Elmer to separate most of the peaks. This method was used for separation of symmetrical peaks by measuring areas of the lower temperature half of peak A_1 and higher temperature half of peak A_2. These half areas were doubled to give each peak area. In cases where the peaks were not symmetrical, a double Gaussian resolution method was adopted. In this method, the endothermic peak is described to be of a 3-parameter Gaussian form:

$$y = ae^{\left(-0.5\left(\frac{x-x_0}{b}\right)^2\right)} \tag{11}$$

where y is the heat flow, x is temperature, a is the maximum height of the peak, b is the mid-height width, and x_0 is the peak center position. The area under a Gaussian curve is

$$y = ab\sqrt{2\pi} \tag{12}$$

The double Gaussian equation used to simulate the two relaxation peaks is:

$$y = ae^{\left(-0.5\left(\frac{x-x_0}{b}\right)^2\right)} + ce^{\left(-0.5\left(\frac{x-x_1}{d}\right)^2\right)} \tag{13}$$

The parameters a and c are the maximum heights of the peaks, b and d are the mid-height widths and x_0 and x_1 are the peak center positions. After obtaining parameters a, b, c, and d by curve fitting, each peak area was calculated. Results obtained using the two different methods were found to be in good agreement, when applied to symmetrical peaks.

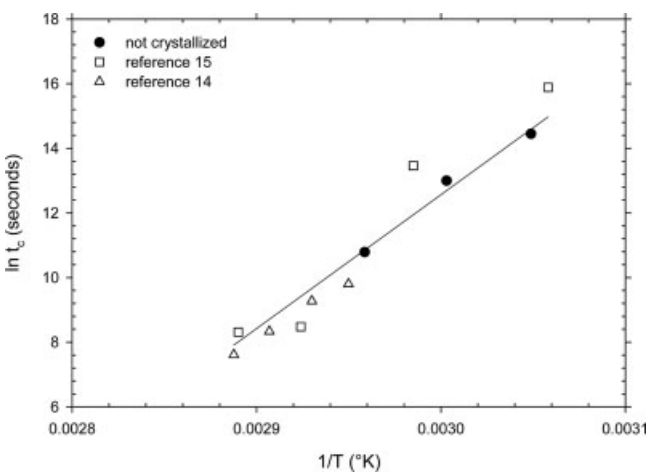

Figure 6 An Arrhenius plot showing characteristic relaxation time values (ln t_c) in terms of the reciprocal of aging temperature. Values from references (Aref-Azar et al.[15] and Bailey et al.[14]) are included.

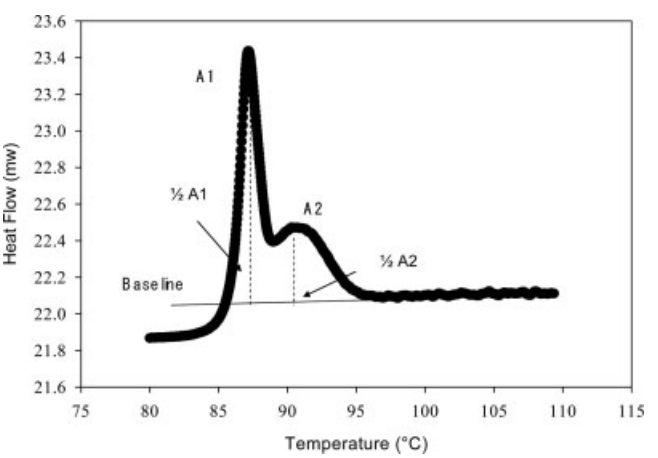

Figure 8 An example of lower temperature interspherulitic (A_1) and higher temperature intraspherulitic (A_2) relaxation endotherms recorded for aged samples of moderate crystallinity.

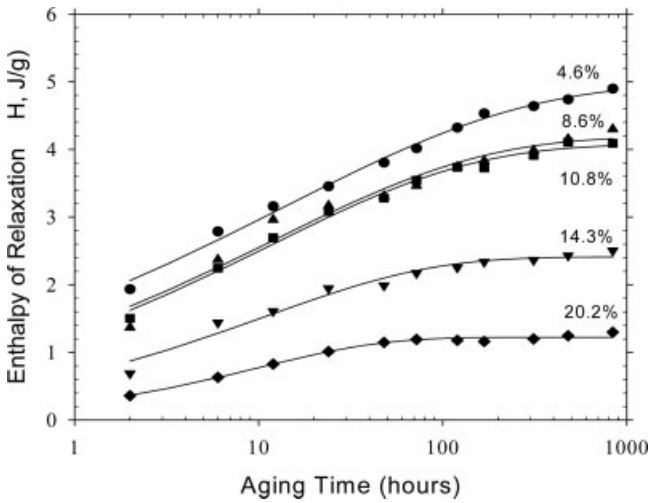

Figure 9 Changes in interspherulitic (A_1) relaxation enthalpy, recorded for samples with levels of crystallinity up to 20.2%, are plotted as functions of aging times at 65°C.

Changes in the enthalpies of relaxation of peak A_1 are shown as functions of aging time in Figure 9. These are changes that occur in the interspherulitic amorphous region. Intraspherulitic changes, represented by peak A_2 are shown in Figure 10. It can be seen that increased aging time results in increased enthalpic relaxation of all amorphous regions. In the case of interspherulitic (A_1) changes, samples with increased crystallinity show decreased peak size, while in the case of intraspherultic (A_2) relaxations, this trend is reversed. Samples with the lowest level of crystallinity do not exhibit peak A_2, while peak A_1 is absent in the case of samples containing 25% crystallinity.

As with the previously described overall endotherm evaluations, the Cowie-Ferguson model was applied to these data. Table IV gives an overview of results obtained from these analyses of peaks A_1 and A_2, for samples aged at 65°C. The relationships of interspherulitic and intraspherulitic relaxation endotherm equilibrium values are shown in Figure 11, plotted as functions of % crystallinity. This plot shows that as levels of crystallinity increase and interspherulitic (A_1) amorphous regions are reduced, maximum equilibrium enthalpy of relaxation values achieved in this region are also reduced. At the same time, it can be seen that maximum intraspherulitic (A_2) values increase with increased levels of crystallinity.

Figure 12 shows the relationships of characteristic relaxation times required for aging within the various amorphous regions. As can be seen, relaxation times obtained for materials within the intraspherulitic regions (A_2) increase greatly, while those for interspherulitic (A_1) regions decrease slightly as levels of crystallinity increase. These slight reductions can be explained in terms of the reduced amorphous phase present between the spherulites. An additional explanation could include the influence of a more mobile, lower molecular weight component, expelled into the interspherulitic region by the advancing crystalline front. The much longer times required for aging within the inter-lamellar amorphous regions of more highly crystalline samples, result from the decreased molecular mobility within these restricted areas. Additional work is in progress to describe the implications of the different behaviors exhibited by interspherulitic and intraspherulitic amorphous regions and their relationships to mechanical properties and environmental stress cracking behaviors.

A number of researchers have used DSC measurements to investigate changes in the positions and intensities of relaxation endotherms exhibited by aged semicrystalline PET. Among these, Zhao et al.[23,24] observed dual endothermic relaxation peaks and attributed their presence to free and constrained amorphous regions within the aged polymer. Montserrat and Cortez[22] as well as Alves et al.[41] have observed lower temperature endotherms believed to result from interspherulitic relaxations and higher temperature endotherms thought to originate from intraspherulitic relaxations. These two separate endotherms were utilized for discussions of the two amorphous regions; however, two glass transitions obtained with DSC were not shown. In additional work Colomer et al.[42] have used thermally stimulated depolarization currents to show three individual relaxations associated with the amorphous interlamellar zone, amorphous regions, and crystalline-amorphous interphases. Current DDSC results provide

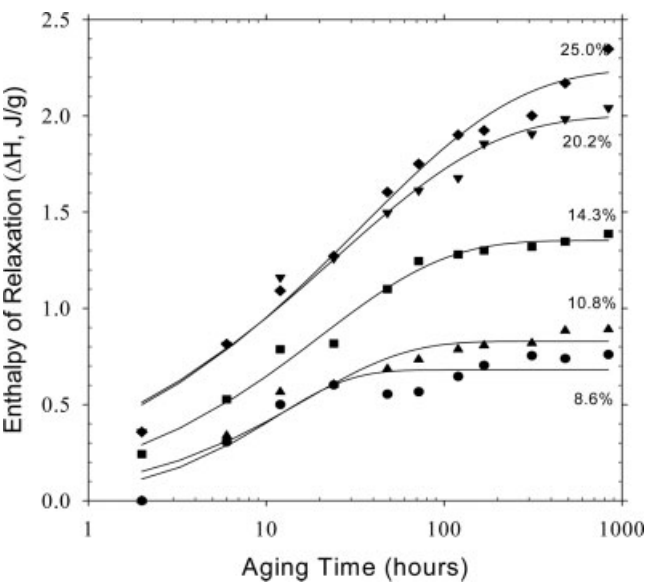

Figure 10 Changes in intraspherulitic (A_2) relaxation enthalpy, recorded for sample with levels of crystallinity from 8.6% to 25.0%, are plotted as functions of aging times at 65°C.

TABLE IV
Interspherulitic and Intraspherulitic Peak Resolution Cowie-Ferguson (CF) Parameters for PET Samples Aged at 65°C

		CF parameters for A_1			CF parameters for A_2		
Density (g/cm^3)	X_c (%)	ΔH_{eq} (J/g)	β	t_c (h)	ΔH_{eq} (J/g)	β	t_c (h)
1.3290	4.6	5.29	0.36	13.5	–	–	–
1.3344	8.6	4.19	0.38	11.8	0.68	1.0	11.1
1.3372	10.8	4.07	0.39	11.5	0.83	0.76	16.5
1.3419	14.3	2.41	0.48	10.6	1.35	0.61	20.1
1.3496	20.2	1.22	0.64	10.0	2.00	0.49	24.7
1.3560	25.0	–	–	–	2.24	0.49	33.9

additional evidence to support the existence of interspherulitic and intraspherulitic amorphous regions. Figure 13(a) shows change in specific heat as a function of temperature for an unaged noncrystallized sample. This material exhibits a clear step change in baseline at T_g (77°C) as indicated by the single well-defined peak of the specific heat derivative. Results shown in Figure 13(b) were obtained for an unaged sample containing 25% crystallinity. In this case, a broad glass transition region, with two-step changes can be observed. These individual transitions are shown more clearly by the two peaks of the specific heat derivative. The lower temperature (77°C) transition corresponds to the interspherulitic amorphous region, while the smaller, higher temperature (83°C) transition arises from the more restricted interlamellar amorphous regions.

SUMMARY AND CONCLUSIONS

The current study has utilized samples of PET, with levels of crystallinity up to 25%, to investigate their aging characteristics at temperatures from 55 to 65°C. Changes in relaxation endotherms have been examined, using DSC and modeled to yield relaxation times and equilibrium relaxation values. Additional evaluations have included specific heat measure-

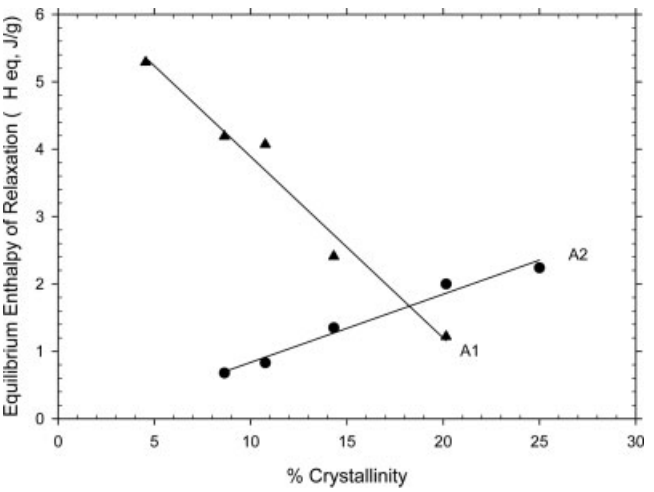

Figure 11 Equilibrium relaxation endotherm values for interspherulitic (A_1) and intraspherulitic (A_2) regions are plotted as functions of % crystallinity.

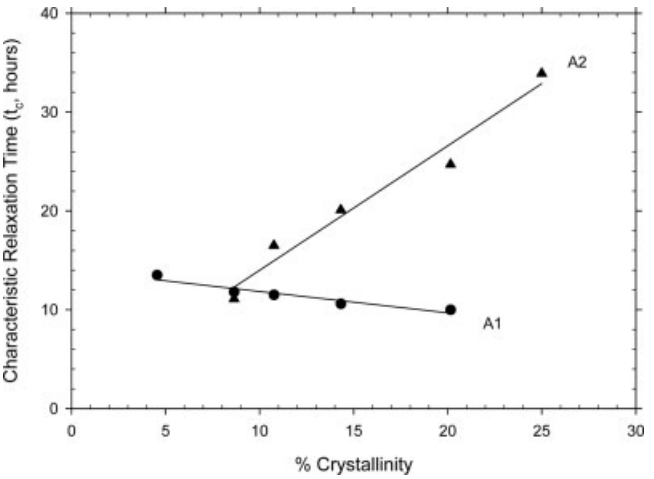

Figure 12 Characteristic relaxation times obtained for interspherulitic (A_1) and intraspherulitic (A_2) regions are plotted as functions of % crystallinity.

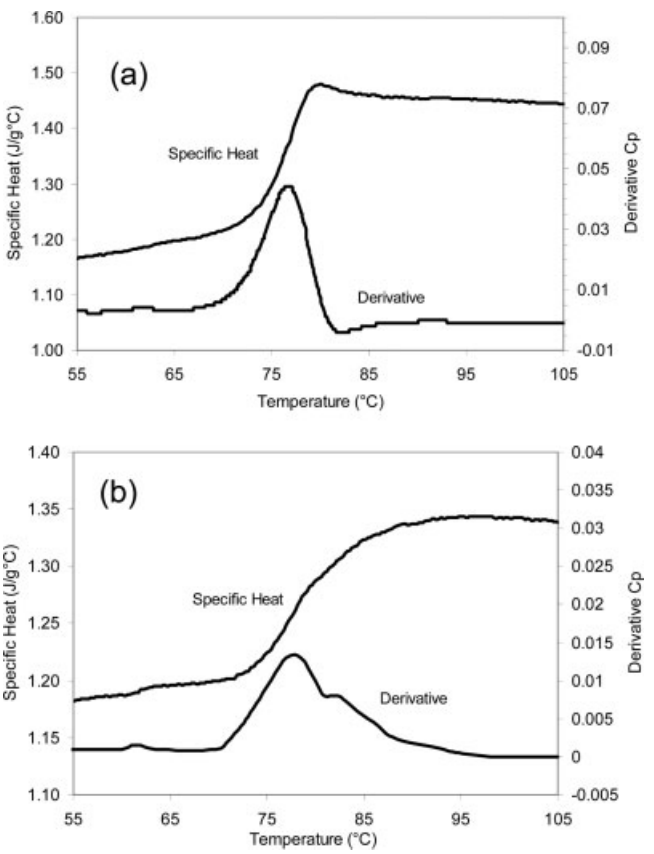

Figure 13 DDSC specific heat results are shown plotted as functions of temperature, illustrating: (a) a single T_g and its derivative for noncrystallized PET and (b) a double T_g and its derivative for a sample of 25% crystallinity.

ments, small angle light scattering analysis, and DDSC. Results show specific individual relaxations of the two amorphous phases and two separate glass transition temperatures. The interspherulitic and intraspherulitic amorphous regions each exhibit separate characteristic relaxation times and equilibrium relaxation values. In addition, specific heat measurements confirm the validity of extrapolating aging data to lower temperatures of aging. Specific conclusions resulting from this work are given below.

1. Changes in overall enthalpy of relaxation values are reduced by increased sample crystallinity and accelerated by increased aging temperature.
2. The Cowie-Ferguson model fits data obtained for physical aging under conditions of combined and separated influences of interspherulitic and intraspherulitic relaxations.
3. Specific heat changes show the validity of equilibrium relaxation endotherm values, obtained with the Cowie-Ferguson model and through extrapolation to lower temperatures.
4. Activation energies for relaxation increase from 337 to 361 kJ/mole as sample crystallinities increase from 4.6 to 25%.
5. Interspherulitic amorphous regions (A_1) give lower equilibrium relaxation endotherms as levels of sample crystallinity increase, while intraspherulitic amorphous regions (A_2) give correspondingly higher equilibrium relaxation endotherms. These differences follow changes in distributions of amorphous contents, from outside the spherulites to within them.
6. At higher levels of sample crystallinity, characteristic relaxation times obtained for interspherulitic amorphous regions decrease very slightly, while those of intraspherulitic amorphous regions increase greatly.
7. Dynamic DSC results for a sample with 25% crystallinity show the presents of two glass transition temperatures, corresponding to interspherulitic and intraspherulitic amorphous regions. A single interspherulitic transition is exhibited by a noncrystallized sample.

References

1. Tant, M. R.; Wilkes, G. L. Polym Eng Sci 1981, 21, 874.
2. Struik, L. C. E. Physical Aging of Amorphous Polymers and Other Materials; Elsevier: New York, 1978.
3. Siegman, A.; Turi, E. J Macromol Sci Phys 1974, 10, 689.
4. Mininni, R. M.; Moore, R. S.; Flick, J. R.; Petrie S. E. B. J Macromol Sci Phys 1973, 8, 343.
5. Aref-Azar, A.; Biddlestone, F.; Hay, J. N.; Haward, R. N. Polymer 1983, 24, 1245.
6. Aref-Azar, A.; Hay, J. N. Polymer 1982, 23, 1129.
7. Moore, R. S.; O'Loanne, J. K.; Shearer, J. C. Polym Eng Sci 1981, 21, 903.
8. Atkinson, J. R.; Biddlestone, F.; Hay J. N. Polymer 2000, 41, 6965.
9. Petrie, S. E. B. In Physical Structure of the Amorphous State; Allen, G.; Petrie, S. E. B., Eds.; Marcel Dekker: New York, 1977; pp 225–247.
10. Jabarin, S. A.; Lofgren, E. A. Polym Eng Sci 1992, 32, 146.
11. Tant, M. R.; Moskala, E. J.; Jank, M. K.; Pecorini, T. J.; Hill, A. J. In Structure and Properties of Glassy Polymers; Tant, M. R.; Hill, A. J., Eds.; ACS: Wahsington, DC, 1998; Chapter 17, pp 242–257. ACS Symp Ser 710.
12. Jabarin, S. A.; Lofgren, E. A.; Sakumoto, S. In Handbook of Thermoplastic Polyesters, Vol. 2: Homopolymers, Copolymers, Blends, and Composites; Fakirov, S., Ed.; Wiley-VCH Verlag GmbH: Weinheim, 2002; Chapter 22, pp 965–1089.
13. Ellis, A.; Gordon, D.; King, S.; Jenkins, M. Sci Direct: Phys B 2006, 385/386, 514.
14. Bailey, N. A.; Hay, J. N.; Price, D. M. Thermochim Acta 2001, 367/368, 425.
15. Aref-Azar, A.; Arnoux, F.; Biddlestone, F.; Hay, J. N. Thermochim Acta 1996, 273, 217.
16. Boyer, R. F. J Polym Sci Symp 1975, 50, 189.
17. Groenincky, G.; Berghmans, H.; Smets, G. J Polym Sci Polym Phys Ed 1976, 14, 591.
18. Newman, S.; Cox, W. P. J Polym Sci 1960, XLVI, 29.
19. Illers, K. H.; Breuer, H. J Colloid Sci 1963, 18, 1.
20. Ito, E. J Polym Sci Polym Phys Ed 1974, 12, 1477.
21. Lee, S. C.; Min, B. G. Polymer 1999, 40, 5445.
22. Montserrat, S.; Cortes P. J Mater Sci 1995, 30, 1790.
23. Zhao, J.; Song, R.; Zhang, Z.; Linghu, X.; Zheng, Z.; Fan, Q. Macromolecules 2001, 34, 343.
24. Zhao, J.; Wang, J.; Li, C.; Fan, Q. Macromolecules 2002, 35, 3097.
25. Bhardwaj, S. Physical Aging Characteristics of PETG, Master Thesis; Polymer Institute, University of Toledo: Toledo, OH, 1999.
26. Angle, R. Physical Aging of Polyesters, Master Thesis; Polymer Institute, University of Toledo: Toledo, OH, 1998.
27. Sakumoto, S. Physical Aging and Environmental Stress Cracking of PET/PEN Blends, Master Thesis; Polymer Institute, University of Toledo: Toledo, OH, 1999.
28. Mukherjee, S.; Jabarin, S. A. ANTEC 1993, 1683.
29. Mukherjee, S.; Jabarin, S. A. ANTEC 1995, 1145.
30. Jabarin, S. A.; Lofgren, E. A.; Mukherjee, S. ANTEC 1994, 3271.
31. Mukherjee, S.; Jabarin, S. A. Polym Eng Sci 1995, 35, 1145.
32. Zhou, H. Effects of Microcrystallinity on Physical Aging and Environmental Stress Cracking of Poly(ethylene terephthalate) (PET), PhD Thesis; Polymer Institute, University of Toledo: Toledo, OH, 2005.
33. Boyd, T. Effects of Copolymerization on the Heat Set Properties of Poly(ethylene terephthalate), Master Thesis; Polymer Institute, University of Toledo: Toledo, OH, 1995.
34. Bunn, C. W.; Daubeny, R. P. Proc R Soc London Ser A 1954, 226, 531.
35. Schawe, J. E. K. J Polym Sci Part B: Polym Phys 1998, 36, 2165.
36. Reading, M. Trends Polym Sci 1993, 1, 248.
37. Stein, R. S.; Rhodes, M. B. J Appl Phys 1960, 31, 1873.
38. Petrie, S. E. B. J Polym Sci Part A-2: Polym Phys 1972, 10, 1255.
39. Cowie, J. M. G.; Ferguson, R. Macromolecules 1989, 22, 2307.
40. Cowie, J. M. G.; Ferguson, R. Macromolecules 1989, 22, 2312.
41. Alves, N. M.; Mano, J. F.; Balaguer, E.; Meseguer Duenas, J. M.; Gomez Ribelles, J. L. Polymer 2002, 43, 4111.
42. Colomer, P.; Monserrat, S.; Belana, J. J Mater Sci 1998, 33, 1921.